# *Moringa Oleifera* Based Electrode Effect on Bacteria for Glucose Oxidation

**Oubaouz Mohamed[1*], Niraka Blaise[2] and Abdelilah Chtaini[1]**

[1]*Molecular Electrochemistry and Inorganic Material Team, LGI-IS, Faculty of Science and Technology Beni Mellal, Morocco*
[2]*National Advanced School of Engineering, University of Maroua, P.O. Box 46, Maroua, Cameroon*
*Corresponding author: m.oubaouz@usms.ma

Received 21/04/2023; accepted 20/06/2023
https://doi.org/10.4152/pea.2024420505

**Abstract**
PA is a gram-negative pathogen that is highly aggressive and known to cause several nosocomial infections, leading to significant morbidity and mortality levels. Individuals with compromised immunity are especially vulnerable to life-threatening infections caused by this bacterium. PA importance as a pathogen is further underscored by its virulence, increasing resistance to antibiotics, and its ability to adapt to diverse environmental conditions. In this study, MO extract antibacterial activity was evaluated using Ec methods, such as CV, EIS and polarization curves (Tafel's law), against pathogenic bacteria, including PA. The performance of the developed CPE modified by MO was herein tested with $C_6H_{12}O_6$, by CV technique. The CV recorded at the CPE-MO surface showed a well-defined peak, which was due to $C_6H_{12}O_6$ Ec oxidation. PA addition to the electrolyte solution containing $C_6H_{12}O_6$ caused its oxidation peak to disappear. The hypothesis that PA would adhere to the CPE-MO surface, blocking the active sites and, subsequently, $C_6H_{12}O_6$ oxidation, was proposed. To verify this hypothesis, polarization curves and EIS, which revealed the presence of a non-conductive film on the CPE-MO surface, were employed. The morphology of the elaborated electrodes surfaces was characterized by SEM.

***Keywords***: CPE; CV; EIS; inhibition; MO; PA; pathogenic bacteria; polarization curve (Tafel's law); SEM; SR.

## Introduction•

### *PA*

PA is a pathogen that can cause severe and even deadly acute or chronic infections. This gram-negative bacterium is classified under the *Pseudomonas* genus, and is also known as *pyocyanin bacillus*, blue pus *bacillus* or *pyocianica* [1].

• The abbreviations list and symbols definition are in page 382.

*PA infections*

PA infections can affect any part of the body such as: respiratory system (pneumonia); heart (endocarditis); central nervous system (meningitis); ears (otitis); eyes, in cornea (keratitis and conjunctivitis, which can even cause total blindness); bones and joints; digestive tract (gastroenteritis); urinary tract infections, which are most often due to hospital instrumentation; and skin (dermatitis and folliculitis).

*PA resistance to antibiotics*

PA is naturally resistant to antibiotics, since it has poor permeability to antibacterial agents, and it also generates enzymes that can degrade antibiotic molecules, like cephalosporins.

*Treatment of pseudomonal infections*

Antibiotics that are effective against PA include carbapenems, certain fluoroquinolones (ciprofloxacin, at high doses), some penicillin types (piperacillin-tazobactam) and third-generation cephalosporins (ceftazidime) (Table 1).

**Table 1:** PA sensitivity to antibiotics [3].

| Antibiotic | Sensitivity | Intermediary | Resistance |
|---|---|---|---|
| Ticarcillin | 54.5% | 14.7% | 30,8% |
| Ceftazidime | 78.6% | 11,6% | 9,8% |
| Imipenem | 72.2% | 12% | 15,8% |
| Ciprofloxacin | 60,4% | 2,3% | 37,3% |
| Amikacin | 75,3% | 10,1% | 14,6% |

Since PA is resistant to antibiotics, infections should be treated by combined therapy [2]. Pseudomonal infections are typically treated using a combination of two antimicrobial agents: beta-lactam and aminoglycoside. Nevertheless, appropriate treatments may depend on the type of infection and affected organs [3], and surgical intervention is rarely needed.

Since antibiotics generally used to treat PA infections have side effects on health, there is the the need to seek an alternative.

***MO***

MO is a versatile, highly adaptable, fast-growing tropical tree that is native to Asia, but also cultivated in Africa, and Central and South America. It belongs to the *Moringa* family, which includes thirteen species (order: *Brassicales*). In recent times, MO has become one of the most important products in pharmaceutical industry [4]. Historically, MO various parts have been traditionally used as food and/or in traditional medicine. Its seeds are known to alleviate the effects of various diseases, particularly inflammatory-mediated conditions, such as cardiovascular and gastrointestinal illnesses, since they have anti-inflammatory, antioxidant, hypotensive, antibacterial and chemo preventive properties [4-6]. Phytochemicals derived from MO seeds have been linked to various bioactivities,

including GLS, ITC, nitriles, carbamates and thiocarbamates presence [5-7]. Bioactive peptides derived from natural plant proteins have recently gained attention in various industries. Lately, natural plant proteins have been extensively sought in health, food preservation and pharmaceutical industries, due to bioactive peptides presence. These peptides typically consist of a chain with 2 to 20 amino acid residues [7, 8]. MO has a reputation as a bactericidal plant, and does not show any chronological toxicity [11].

## Materials and methods

### *Reagents and chemicals*

All chemicals used in this work are of high quality. Gr powder, (spectroscopic grade RWB, Ringsdorff-Werke GmbH, Bonn-Bad Godesberg, Germany), was obtained from Aldrich, and used without further purification. The mother electrode modifying reagent, used in the form of MO powder, was obtained from a Cameron medicine tree. PA bacteria strain is of commercial grade. Deionized water was used to prepare all the solutions.

### *Device*

Ec experiments were conducted using a Voltalab potentiostat (model PGSTAT 100, Eco Chemie BV, Utrecht, The Netherlands), driven by general purpose Ec systems data processing software (Voltalab master 4 software). The measurement cell used in this work was a three-electrode cell. CPE-MO was used as WE, SCE served as RE and Pt plate as AE.

### *Electrodes preparation*

The paste constituting the indicator electrode was a mixture of Gr powder and binder (paraffin) [9]. C paste was then shaped in the cavity of an electrode body, and polished to obtain a flat surface. CPE-MO (crushed) was immersed in a NaCl solution [10].

## Results and discussion

Fig. 1 shows CV recorded at a SR of 50 mV/S, on the CPE surface (curve a) and on the CPE-MO (curve b) surface, respectively, in 1 M NaCl.

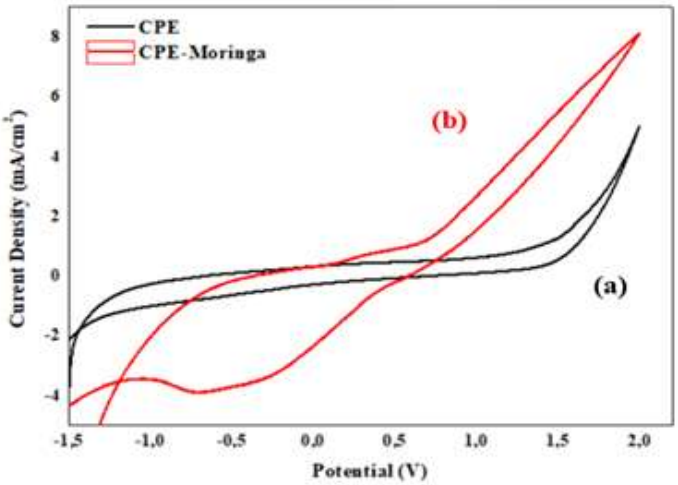


**Figure 1**: CV recorded at 50 mV/s, in NaCl, on: (**a)** CPE; and (**b)** CPE-MO.

The two voltammograms show different shapes, which proves that the mother electrode modification was successful. CPE-MO shows a small oxidation peak at around 0.5 V, and a large peak towards the cathode, at about -0.5 V. The two peaks are sufficiently aligned, indicating that this is not a redox system.
The morphology of the elaborated electrodes surfaces was characterized by SEM. The SEM image of CPE (Fig. 2 (A)) shows a compact surface which presents some defects and relatively deep pores. CPE surface has an irregular structure, with reliefs. CPE-MO surface shows reliefs and porous connections. The pores are very deeply surrounded by large MO surfaces (Fig. 2 (B)).

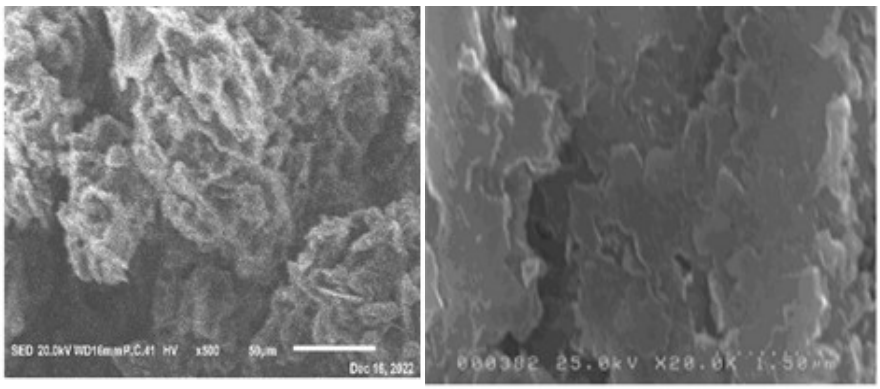

**(A)** **(B)**

**Figure 2:** SEM images: **(A)** CPE; and **(B)** CPE-MO.

Fig. 3 (A) represents CV in the absence (curve a) and presence of $C_6H_{12}O_6$ (curve b). We can notice that $C_6H_{12}O_6$ oxidation was manifested by an anodic peak, which appeared around 0.9 V, towards the anode. This well-defined peak led to MO reduction peaks disappearance, which suggests that its addition to CPE promoted $C_6H_{12}O_6$ oxidation. $C_6H_{12}O_6$ oxidation on the CPE-MO surface remarkable changed its morphology, which seems to consist of large branched rods with deep pores between them (Fig. 3. B).

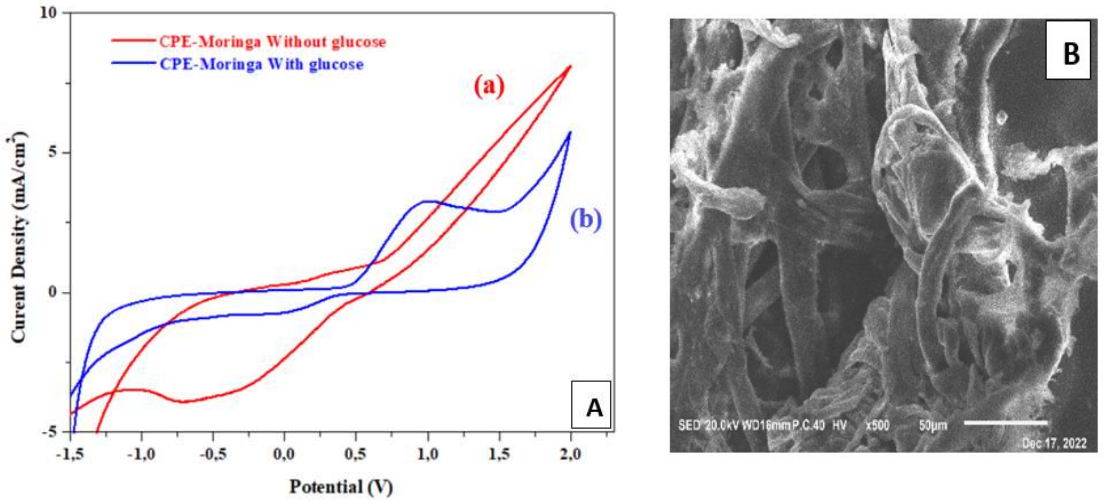


**Figure 3: (A)** CV of GCE and CPE-MO in 1 M NaCl, at 50 $mVs^{-1}$; **(B)** SEM image of CPE-MO with $C_6H_{12}O_6$.

PA addition to 1 M NaCl with $C_6H_{12}O_6$ affected the CV (Fig. 4 (A)). The CV shows that redox peaks disappeared, and $C_6H_{12}O_6$ oxidation was deactivated. These phenomena occurred because the bacteria adhered on to the electrode surface and blocked its active sites. SEM image confirms these observations, and shows a homogeneous and regular structure, without the previously seen batons (Fig. 4 (B)).

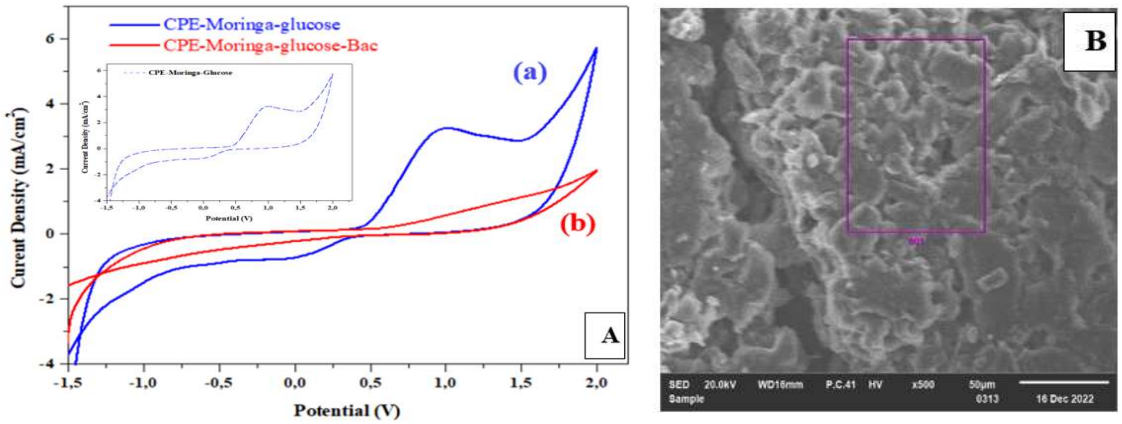


**Figure 4:** Effect of PA in 1 M NaCl with $C_6H_{12}O_6$ on **(A)** GCE-MO, at SR of 50 $mV/s^{-1}$ (CV); and **(B)** CPE-MO (SEM image).

Ct of PA did not affect the CV (Fig. 5) recorded on the modified CPE-MO surface, in 1 M NaCl with $C_6H_{12}O_6$. On the contrary, j values decreased with higher Ct of PA, which confirms the hypothesis that it formed a film on the CPE-MO surface, and blocked its active sites.

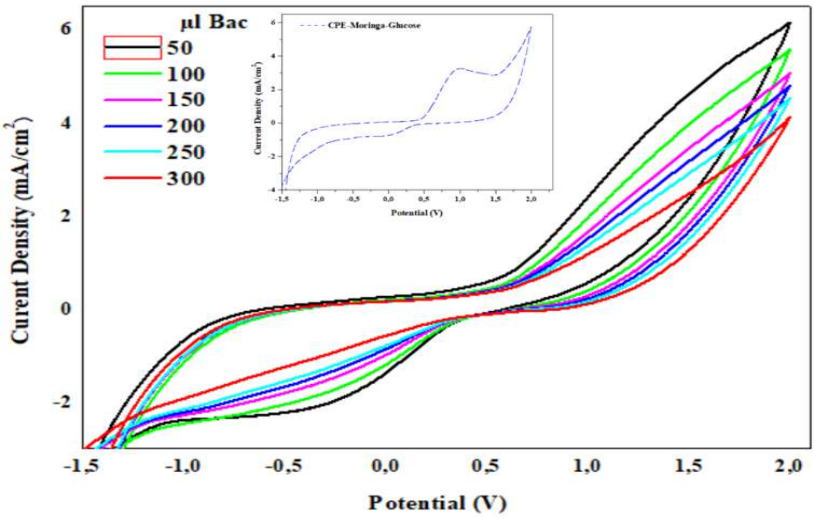


**Figure 5:** CV of GCE and CPE-MO in 1 M NaCl with $C_6H_{12}O_6$, under PA effect.

EIS diagrams in the Nyquist plane (Fig. 6) show the bacteria Ct effect on $C_6H_{12}O_6$ oxidation, at the CPE-MO surface. It is seen that EIS curves have the shape of semi-circles, for all Ct of PA. These curves moved towards low frequencies, which confirms CPE-MO surface conductivity loss. Ec parameters deduced from EIS curves are shown in Table 2. Capacitance values increased considerably with the Ct of PA, which confirms that they formed a dense film on the CPE-MO surface.

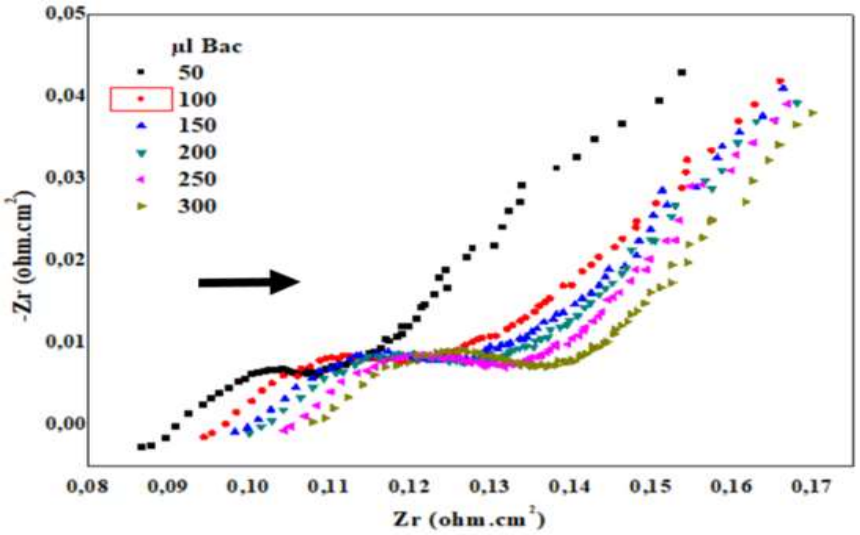


**Figure 6:** EIS of GCE and GCE-MO in 1 M NaCl, under PA effect.

**Table 2:** Ec parameters from EIS.

| PA (µl) | Diameters (ohm/cm²) | Correlation | R¹ (ohm/cm²) | R² (ohm/cm²) | R²-R¹ | Ct (µf/cm²) |
|---|---|---|---|---|---|---|
| 0 | 22.2 | 0.998 | 587.2 | 19.65 | 567.55 | 80.99 |
| 50 | 44.1 | 0.986 | 115.9 | 35.69 | 80.21 | 294 |
| 100 | 44 | 0.983 | 119.2 | 39.23 | 79.97 | 288.7 |
| 150 | 55.7 | 0.986 | 121.2 | 46.54 | 74.66 | 243.4 |
| 200 | 58.6 | 0.979 | 127.2 | 50.85 | 76.35 | 197.7 |
| 250 | 62.2 | 0.980 | 124.4 | 52.16 | 72.24 | 217.2 |

To explain $C_6H_{12}O_6$ oxidation peak disappearance, the polarization curve of CPE-MO in NaCl with PA (Fig. 7) was plotted.

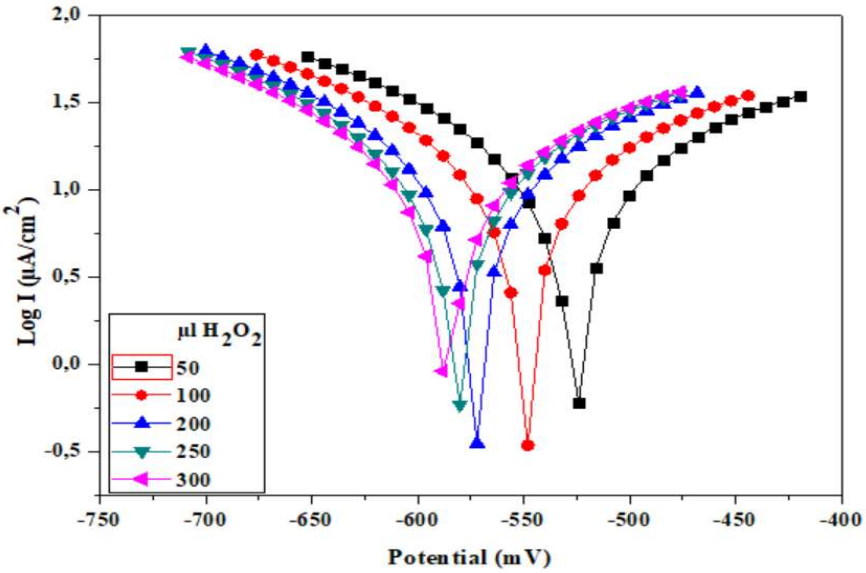


**Figure 7:** Polarization curve (Tafel line) of CPE-MO in 1 M NaCl, under PA effect.

The curve processing allowed to determine Ec parameters (Table 3) such as j and E (I = 0). PA addition to NaCl shifted the equilibrium E towards very negative values, giving relatively lower CR, which supports the hypothesis that a PA film was formed on the CPE-MO surface, hindering $C_6H_{12}O_6$ oxidation.

**Table 3:** Ec parameters from polarization curve.

| PA (µl) | E (I = 0) (K/ohm/cm²) | $R_p$ (K/ohm/cm²) | j | $\beta_a$ (mV) | $\beta_c$ (mV) | $R^2$ | CR (mm/y) |
|---|---|---|---|---|---|---|---|
| 50 | -519.1 | 1.30 | 28.63 | 263.5 | -199.4 | 0.998 | 334.8 |
| 100 | -535.6 | 1.37 | 26.51 | 262.2 | -195.6 | 0.998 | 314.8 |
| 150 | -554.9 | 1, 39 | 26.17 | 261.2 | -190.9 | 0.997 | 306 |
| 200 | -555.7 | 1.42 | 27.30 | 279.1 | -200 | 0.997 | 319.3 |
| 250 | -561.9 | 1.45 | 25.48 | 266.8 | -193 | 0.998 | 298 |
| 300 | -545.1 | 1.46 | 26.17 | 263.8 | -194.9 | 0.998 | 294.4 |
| 350 | -570.2 | 1.49 | 24.87 | 268.3 | -194.1 | 0.998 | 290.9 |

### *CA study of $C_6H_{12}O_6$ oxidation kinetics*

The transients presented in Fig. 8 show a remarkable activity of CPE-MO, concerning $CH_{12}O_6$ oxidation, at the reaction start, for the first 20 min. j decreased as a function of time. These transients were recorded at glycose oxidation E. J values recorded on the plateaus gradually decreased, which means that CPE-MO activity was not affected by PA (Fig. 9).

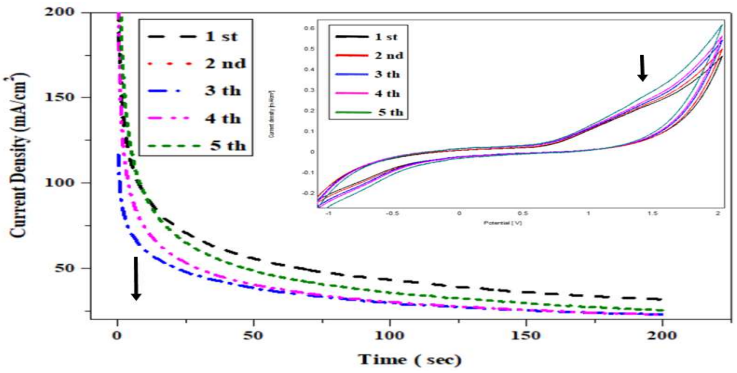


**Figure 8:** Transient curves recorded at CPE-MO, in 1 M NaCl with 0.1 mmol $C_6H_{12}O_6$.

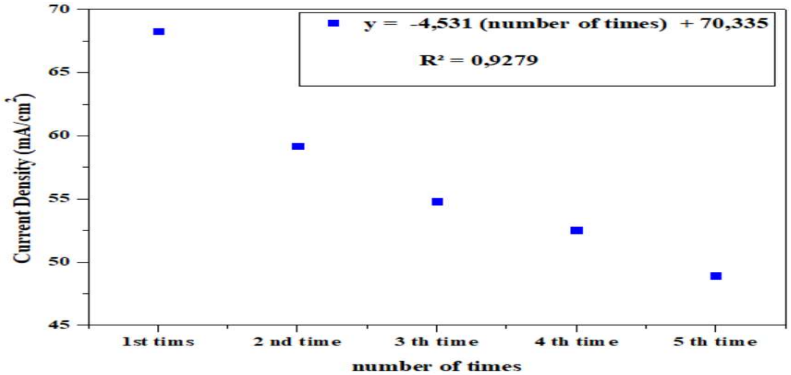


**Figure 9:** CA of CPE-MO j calibration curves, in 1 M NaCl with 0.1 mmol $C_6H_{12}O_6$.

## Conclusion

A CPE-MO was herein developed. Its performance was tested by CV, upon $C_6H_{12}O_6$ oxidation. The CV recorded at the CPE-MO surface showed a well-defined peak, which was due to $C_6H_{12}O_6$ Ec oxidation. PA addition to NaCl with $C_6H_{12}O_6$ eliminated its oxidation peak. The hypothesis that PA would adhere to the CPE-MO surface, blocking its active sites and, subsequently, $C_6H_{12}O_6$ oxidation, was proposed. To verify this hypothesis, polarization curves and EIS, which revealed the presence of a non-conductive film on the CPE-MO surface, were employed.

## Authors' contributions

**Oubaouz Mohamed**: processed data manipulation. **Niraka Blaise**: processed data manipulation. **Abdelilah Chtaini**: analyzed data and addressed the article premise.

## Abbreviations

**AE**: auxiliary electrode
**$C_6H_{12}O_6$**: glucose
**CA**: chronoamperometry
**CPE**: carbon paste electrode
**CR**: corrosion rate
**Ct**: concentration
**CV**: cyclic voltammetry
**E**: potential
**Ec**: electrochemical
**EIS**: impedance spectroscopy
**GCE**: graphite carbon electrode
**GLS**: glucosinolates
**Gr**: graphite
**I**: current
**ITC**: isothiocyanates
**j**: current density
**NaCl**: sodium chloride
**PA**: *Pseudomonas aeruginosa*
**$R^2$**: coefficient of determination
**RE**: reference electrode
**Redox**: reduction/oxidation reaction
**$R_p$**: polarization resistance
**SCE**: saturated calomel electrode
**SEM**: scanning electron microscopy
**SR**: scanning rate
**WE**: working electrode

## Symbols definitions

**βa**: anodic Tafel slope
**βc**: cathodic Tafel slope

## References


1. Mans S, Canouet S. *Pseudomonas aeruginosa*: A water story [archive], on www.cclin-sudouest.com Sud-Ouest Nosocomial Infection Control Coordination Center. 2008.
2. Dr. Alexander Vögtli. PharmaWiki 2007-2023. *PharmaWiki informiert unabhängig und zuverlässig über Medikamente und Gesundheit*.
3. Van Helden C, Iglewski B. Cell-to-cell signaling and *Pseudomonas aeruginosa* infections. Emerging Infectious Disease. 1998;4(4):551-560. https://doi.org/10.3201/eid0404.980405
4. Anwar F, Latif S, Ashraf M et al. *Moringa oleifera*: a food plant with multiple medicinal uses. Phytother Res. 2007;21:17-25. https://doi.org/10.1002/ptr.2023
5. Fahey JW. *Moringa oleifera*: a review of the medical evidence for its nutritional, therapeutic, and prophylactic properties. Part 1. Trees Life J. 2005;1:1-15. https://doi.org/10.1201/9781420039078.ch12
6. Karim NAA, Ibrahim MD, Kntayya SB et al. *Moringa oleifera Lam*: targeting chemoprevention. Asian Pac J Cancer Prev. 2016;17:3675-3686.
7. Fayazuddin M, Ahmad F, Kumar A et al. An experimental evaluation of anti-inflammatory activity of *Moringa oleifera* seeds. Int J Pharm Pharm Sci. 2013;5:717-721.
8. Görgüç A, Gençdağ E, Yılmaz F. bioactive peptides derived from plant- of origin by-products: Biological activities and technical-functional uses in food developments–A Review. Int Food Res. 2020;136:109504. https://doi.org/10.1016/j.foodres.2020.109504
9. Gu X, Yang Y, Wang Z. Nutritional, phytochemical, antioxidant, α-glucosidase and α-amylase inhibitory properties of *Moringa oleifera* seeds. South Afric J Botan. 2020;133:151-160.
10. Oubaouz Mohamed, Smaini Imane, Maallah Raja et al. Zinc Modified Carbon Paste Anode for Microbial Fuel Cells. J Xindian Univ. 2022. https://doi.org/10.37896/jxu16.11/058
11. Jorrit van den Berg and Saskia KuipersDubey. The antibacterial action of *Moringa oleifera*: A systematic review. South Afric J Botan. 2022;151:224-233. https://doi.org/10.1016/j.sajb.2022.09.034